Nakayama T, Nakamura H, Oya Y, Kimura T, Imahuku I, **Ohno K**, Nishino I, Abe K, Matsuura T.	Clinical and genetic analysis of the first known Asian family with myotonic dystrophy type 2	*J Hum Genet*	59	129-133	2014
Kokunai Y*, Nakata T*, Furuta M*, Sakata S, Kimura H, Aiba T, Yoshinaga M, Osaki Y, Nakamori M, Itoh H, Sato T, Kubota T, Kadota K, Shindo K, Mochizuki H, Shimizu W, Horie M, Okamura Y, **Ohno K**, Takahashi M. *Equal contribution.	A Kir3.4 mutation causes Andersen-Tawil syndrome by an inhibitory effect on Kir2.1	*Neurology*	82	1058-1064	2014
Mano Y, Kotani T, Ito M, Nagai T, Ichinohashi Y, Yamada K, **Ohno K**, Kikkawa F, Toyokuni S.	Maternal molecular hydrogen administration ameliorates rat fetal hippocampal damage caused by in utero ischemia-reperfusion	*Free Radic Biol Med*	69	324-330	2014
Takamatsu A, Ohkawara B, Ito M, Masuda A, Sakai T, Ishiguro N, **Ohno K**.	Verapamil protects against cartilage degradation in osteoarthritis by inhibiting Wnt/β-catenin signaling	*PLOS ONE*	9	e92699	2014
Kobayashi M, Ohno T, Ihara K, Murai A, Kumazawa M, Hoshino H, Iwanaga K, Iwai H, Hamana Y, Ito M, **Ohno K**, Horio F.	Searching for genomic region of high-fat diet-induced type 2 diabetes in mouse chromosome 2 by analysis of congenic strains	*PLOS ONE*	9	e96271	2014
Yamashita Y*, Matsuura T*, Kurosaki T, Amakusa Y, Kinoshita M, Ibi T, Sahashi K, **Ohno K**. *Equal contribution.	LDB3 splicing abnormalities are specific to skeletal muscles of patients with myotonic dystrophy type 1 and alter its PKC binding affinity	*Neurobiol Disord*	69	200-205	2014
Asai N, Ohkawara B, Ito M, Masuda A, Ishiguro N, **Ohno K**	LRP4 induces extracellular matrix productions and facilitates chondrocyte differentiation	*Biochem Biophys Res Commun*	451	302-307	2014
Nasrin F, Rahman MA, Masuda A, Ohe K, Takeda J, **Ohno K.**	HnRNP C, YB-1 and hnRNP L coordinately enhance skipping of human MUSK exon 10 to generate a Wnt-insensitive MuSK isoform.	*Sci Rep*	4	6841	2014
Nishizaki, Y., Takagi, T., Matsui, F. and **Higashi, Y.**	SIP1 expression patterns in brain investigated by generating a SIP1-EGFP reporter knock-in mouse	*Genesis*	52	56-67	2014
Kimura, M,, Machida, J., Yamaguchi, S., Shibata, S., Tatematsu, T., Miyachi, H., Peter A. Jezewski, P. A., Nakayama, A., **Higashi, Y.**, Shimozato, K. and Tokita, Y.	Novel nonsense mutation in MSX1 in familial nonsyndromic oligodontia: subcellular localization and role of homeodomain/MH4	*Eur J Oral Sci*	122	15-20	2014

Yamaguchi S, Machida J, Kamamoto M, Kimura M, Shibata A, Tatematsu T, Miyachi H, **Higashi Y**, Jezewski P, Nakayama A, Shimozato K, Tokita Y.	Characterization of novel MSX1 mutations identified in Japanese patients with nonsyndromic tooth agenesis.	*PLoS One*	9	e102944	2014
Zhang Y, **Haga N.**	Skeletal compli-cations in congenital insensitivity to pain with anhidrosis: a case series of 14 patients and review of articles published in Japanese	*J Orthop Sci*	19	827-831	2014
Okabe YT, Kondo T, Mishima K, Hayase Y, Kato K, Mizuno M, Ishiguro N, **Kitoh H.**	Biodistribution of locally or systemically transplanted osteoblast-like cells.	Bone Joint Res	3	76-81	2014
Azuma Y, Nakata T, Tanaka M, Shen XM, Ito M, Iwata S, Okuno T, Nomura Y, Ando N, Ishigaki K, Ohkawara B, Masuda A, Natsume J, Kojima S, Sokabe M, **Ohno K.**	Congenital myasthenic syndrome in Japan: Ethnically unique mutations in muscle nicotinic acetylcholine receptor subunits	*Neuromuscular Disorders*	25	60-69	2015
Matsushita M, Hasegawa S, Kitoh H, Mori K, Ohkawara B, Yasoda A, Masuda A, Ishiguro N, **Ohno K.**	Meclozine promotes longitudinal skeletal growth in transgenic mice with achondroplasia carrying a gain-of-function mutation in the FGFR3 gene.	*Endocrinology*	156	548-554	2015
Funayama M, Ohe K, Amo T, Furuya N, Yamaguchi J, Saiki S, Li Y, Ogaki K, Ando M, Yoshino H, Tomiyama H, Nishioka K, Hasegawa K, Saiki H, Satake W, Mogushi K, Sasaki R, Kokubo Y, Kuzuhara S, Toda T, Mizuno Y, Uchiyama Y, **Ohno K**, Hattori N	CHCHD2 mutations in autosomal dominant late-onset Parkinson's disease: a genome-wide linkage and sequencing study	*Lancet Neurol*	14	274-282	2015
Tsunoda M, Hirayama M, Tsuda T, **Ohno K**.	Noninvasive monitoring of plasma l-dopa concentrations using sweat samples in Parkinson's disease	*Clin Chim Acta*	442	52-55	2015
Sobue S, Yamai K, Ito M, **Ohno K**, Iwamoto T, Qiao S, Ohkuwa T, Ichihara M.	Simultaneous oral and inhalational intake of molecular hydrogen additively suppresses signaling pathways in rodents	*Mol Cell Biochem*	403	231-241	2015
Masuda A, Takeda J, Okuno T, Okamoto T, Ohkawara B, Ito M, Ishigaki S, Sobue G, **Ohno K**.	Position-specific binding of FUS to nascent RNA regulates mRNA length	*Genes Dev*	29	1045-1057	2015
Selcen D, Ohkawara B, Shen X-M, McEvoy K, **Ohno K**, Engel AG.	LRP4 myasthenia. Impaired Synaptic Development, Maintenance, and Neuromuscular Transmission in LRP4 Myasthenia	*JAMA Neurology*		in press	
Udagawa T, Fujioka Y, Tanaka M, Honda D, Yokoi S, Riku Y, Ibi D, Nagai T, Yamada K, Watanabe H, Katsuno M, Inada T, **Ohno K**, Sokabe M, Okado H, Ishigaki S, Sobue G.	FUS regulates AMPA receptor function and FTLD/ALS-associated behavior via GluA1 mRNA stabilization	*Nat Commun*		in press	
Fujii H, Matsubara K, Sakai K, Ito M, **Ohno K**, Ueda M, Yamamoto A.	Dopaminergic differentiation of stem cells from Human deciduous teeth and their therapeutic benefits for parkinsonian rats	*Brain Res*		in press	

Iwata S, Ito M, Nakata T, Noguchi Y, Okuno T, Ohkawara B, Masuda A, Goto T, Adachi M, Osaka H, Nonaka R, Arikawa-Hirasawa E, **Ohno K**.	A missense mutation in domain III in *HSPG2* in Schwartz-Jampel syndrome compromises secretion of perlecan into the extracellular space	*Neuromuscular Disorders*		in press	
Kishimoto Y, Kato T, Ito M, Azuma Y, Fukasawa Y, **Ohno K**, Kojima S.	Molecular hydrogen ameliorates monocrotaline-induced pulmonary hypertension in rats by modulating the STAT3/NFAT axis with anti-inflammatory and anti-oxidative effects	*J Thorac Cardiov Surg*		in press	
芳賀信彦	小児運動器疾患のリハビリテーション:現状と展望	東北医学雑誌	124 (1)	38-40	2012
芳賀信彦、田中信幸、田中弘志	先天性無痛無汗症の治療戦略	日整会誌	87	57-60	2013
柳田晴久	症候性側弯症	小児科診療	Vol.78 No.4, 2015	529-535	2015

研究成果の刊行物・別刷

RESEARCH ARTICLE

Human Mutation

OFFICIAL JOURNAL
HGVS
HUMAN GENOME VARIATION SOCIETY
www.hgvs.org

Mutations in the C-Terminal Domain of ColQ in Endplate Acetylcholinesterase Deficiency Compromise ColQ–MuSK Interaction

Tomohiko Nakata,[1,2] Mikako Ito,[1] Yoshiteru Azuma,[1,2] Kenji Otsuka,[1] Yoichiro Noguchi,[1] Hirofumi Komaki,[3] Akihisa Okumura,[4] Kazuhiro Shiraishi,[5] Akio Masuda,[1] Jun Natsume,[2] Seiji Kojima,[2] and Kinji Ohno[1]*

[1]*Division of Neurogenetics Center for Neurological Diseases and Cancer, Nagoya University Graduate School of Medicine, Nagoya, Japan;* [2]*Department of Pediatrics Nagoya University Graduate School of Medicine, Nagoya, Japan;* [3]*Department of Child Neurology National Center Hospital, National Center of Neurology and Psychiatry (NCNP), Tokyo, Japan;* [4]*Department of Pediatrics Juntendo University Faculty of Medicine, Tokyo, Japan;* [5]*Department of Pediatrics Utano National Hospital, Kyoto, Japan*

Communicated by Lars Bertram

Received 19 January 2013; accepted revised manuscript 19 March 2013.
Published online 29 March 2013 in Wiley Online Library (www.wiley.com/humanmutation). DOI: 10.1002/humu.22325

ABSTRACT: Acetylcholinesterase (AChE) at the neuromuscular junction (NMJ) is mostly composed of an asymmetric form in which three tetramers of catalytic AChE subunits are linked to a triple helical collagen Q (ColQ). Mutations in *COLQ* cause endplate AChE deficiency. We report three patients with endplate AChE deficiency with five recessive *COLQ* mutations. Sedimentation profiles showed that p.Val322Asp and p.Arg227X, but not p.Cys444Tyr, p.Asp447His, or p.Arg452Cys, inhibit formation of triple helical ColQ. In vitro overlay of mutant ColQ-tailed AChE on muscle sections of *Colq*$^{-/-}$ mice revealed that p.Cys444Tyr, p.Asp447His, and p.Arg452Cys in the C-terminal domain (CTD) abrogate anchoring ColQ-tailed AChE to the NMJ. In vitro plate-binding assay similarly demonstrated that the three mutants inhibit binding of ColQ-tailed AChE to MuSK. We also confirmed the pathogenicity of p.Asp447His by treating *Colq*$^{-/-}$ mice with adeno-associated virus serotype 8 carrying mutant *COLQ*-p.Asp447His. The treated mice showed no improvement in motor functions and no anchoring of ColQ-tailed AChE at the NMJ. Electroporation of mutant *COLQ* harboring p.Cys444Tyr, p.Asp447His, and p.Arg452Cys into anterior tibial muscles of *Colq*$^{-/-}$ mice similarly failed to anchor ColQ-tailed AChE at the NMJ. We proved that the missense mutations in ColQ–CTD cause endplate AChE deficiency by compromising ColQ–MuSK interaction at the NMJ.
Hum Mutat 34:997–1004, 2013. © 2013 Wiley Periodicals, Inc.

KEY WORDS: COLQ; collagen Q; neuromuscular; acetylcholinesterase; myasthenic syndromes

Introduction

Congenital myasthenic syndromes (CMS) are clinically and genetically heterogeneous inherited disorders characterized by neuromuscular transmission defect caused by mutations affecting proteins expressed at the neuromuscular junction (NMJ) [Engel et al., 2003]. The synaptic type of CMS is caused by the absence of the asymmetric form of acetylcholinesterase (AChE) from the endplate [Engel et al., 1977]. Endplate AChE deficiency is characterized by generalized muscle weakness, fatigue, scoliosis, minor facial abnormalities, and episodes of respiratory distress [Mihaylova et al., 2008]. In the absence of AChE, the duration of the endplate currents are prolonged, so that it outlasts the refractory period of the skeletal muscle sodium channel, which in turn evokes repetitive compound muscle action potentials (CMAPs). Four mechanisms lead to defective neuromuscular signal transmission in endplate AChE deficiency [Engel et al., 1977; Ohno et al., 1998]. First, the prolonged endplate currents lead to overload of Ca^{2+} ions at the postsynaptic sarcoplasm, which causes endplate myopathy with loss of acetylcholine receptor (AChR). Second, excessive ACh at the synaptic space causes desensitization of AChR. Third, repeated opening of AChR causes staircase summation of endplate potentials, which depolarizes the resting membrane potential and makes the muscle sodium channel irresponsive to an endplate potential. Fourth, lack of ColQ at the NMJ diminishes the amount of membrane-bound MuSK and reduces phosphorylation of the AChR β subunit, which compromises AChR clustering [Sigoillot et al., 2010]. Lack of effects of cholinesterase inhibitors, or even worsening of the symptoms with them, in patients with endplate AChE deficiency suggests that lack of AChE rather than lack of AChR is a key underlying mechanism leading to myasthenic symptoms.

Endplate AChE deficiency is not caused by mutations in the *ACHE* gene (NM_000665.3; MIM #100740) encoding the catalytic subunit but is caused by recessive mutations in the *COLQ* gene (NM_005677.3; MIM #603033) encoding the collagenic tail subunit [Ohno et al., 1998]. There are two major types of AChE in the skeletal muscle: (1) globular forms consisting of monomers (G_1), dimmers (G_2), or tetramers (G_4) of the T isoform of the catalytic subunit ($AChE_T$, NP_000656.1), and (2) asymmetric forms consisting of one, two, or three homotetramers (A_4, A_8 and A_{12}, respectively) of $AChE_T$ attached to a triple-stranded collagenic tail (ColQ) [Massoulie, 2002], which are hereafter called ColQ-tailed

Additional Supporting Information may be found in the online version of this article.

*Correspondence to: Kinji Ohno, Division of Neurogenetics, Center for Neurological Disease and Cancer, Nagoya University Graduate School of Medicine, 65 Tsurumai, Showa-ku, Nagoya 466-8550, Japan. E-mail: ohnok@med.nagoya-u.ac.jp

Contract grant sponsors: Ministry of Education, Culture, Sports, Science, and Technology of Japan, and the Ministry of Health, Labor, and Welfare of Japan.

AChE species. ColQ carries three domains: (1) an N-terminal proline-rich attachment domain that organizes the catalytic AChE subunits into a tetramer, (2) a collagen domain that forms a triple helix and contains heparin-binding domains, and (3) a C-terminal domain (CTD) enriched in charged residues and cysteines.

In previous studies, *COLQ* mutations were divided into- four classes according to their positions in ColQ and their effects on the expression of AChE species in COS cells: (1) N-terminal mutations that prevent association of $AChE_T$ with ColQ, (2) truncation mutations in the collagen domain that prevent the formation of ColQ-tailed AChE, (3) CTD missense mutations that prevent triple helical formation of ColQ, and (4) CTD mutations that do not abolish formation of ColQ-tailed AChE but affect anchoring of ColQ at the NMJ [Ohno et al., 2000]. We previously reported that p.Asp342Glu, p.Arg410Pro, and p.Arg410Glu, but not p.Cys444Tyr, at the CTD of ColQ compromise anchoring ColQ-tailed AChE to heterologous frog muscle sections [Kimbell et al., 2004]. We, however, did not show how the mutations affect anchoring of ColQ to the synaptic basal lamina. We also failed to prove pathogenicity of p.Cys444Tyr in the heterologous anchoring experiment. Two binding partners for anchoring ColQ-tailed AChE at the synaptic basal lamina have been reported to date: (1) the heparan sulfate proteoglycans such as perlecan, which bind to two heparan sulfate proteoglycan binding domains in the ColQ collagen domain [Arikawa-Hirasawa et al., 2002], and (2) the extracellular domain of MuSK, a muscle-specific receptor tyrosine kinase, on the postsynaptic membrane, which binds to the CTD of ColQ [Cartaud et al., 2004]. We recently demonstrated that anti-MuSK autoantibodies in patients with myasthenia gravis block binding of ColQ to MuSK [Kawakami et al., 2011]. We also reported that intravenous or intramuscular administration of adeno-associated virus serotype 8 (AAV8) carrying human *COLQ* efficiently anchors ColQ-tailed AChE at the NMJ [Ito et al., 2012]. We proved that ColQ-tailed AChE moves from one muscle to another and anchors to the synaptic basal lamina by exploiting the proprietary binding affinity for synaptic basal lamina, which we named the protein-anchoring therapy.

We here report three patients with AChE deficiency harboring *COLQ* mutations in the collagen domain and CTD. We examined the effects of the CTD mutations on interaction between ColQ and MuSK by in vitro and in vivo assays and found that the CTD mutations impair this interaction.

Materials and Methods

Patients

All human studies were performed under approvals of the institutional review boards of Nagoya University Graduate School of Medicine, National Center of Neurology and Psychiatry, Juntendo University Faculty of Medicine, and Utano National Hospital. Three patients participated in the study after appropriate informed consents were given. A mutation analysis had been done when they were 7, 12, and 19 years of age, respectively. All had respiratory distress or poor sucking at birth, slight delay in walking, fatigability since early childhood, normal intelligence, no anti-AChR and anti-MuSK antibodies, a decremental electromyographic response, repetitive CMAP to a single nerve stimulus, and no response to anticholinesterase medications (Table 1).

Mutation Analysis

Genomic DNA was isolated from blood with QIAamp Blood Mini Kit (Qiagen, Hilden, Germany). Poor response to anticholinesterases suggested endplate AChE deficiency and slow channel syndrome. We thus directly sequenced 17 constitutive *COLQ* exons and their flanking regions with CEQ8000 sequencer (Beckman Coulter, Brea, CA). Names of all mutations were checked using Mutalyzer (http://www.lovd.nl/mutalyzer/). Identified mutations were submitted to an LSDB for the *COLQ* gene (http://www.lovd.nl/COLQ). As mutations were identified in *COLQ* in all the patients, we did not go into sequencing of *CHRNA1* (NM_00079.3; MIM #100690), *CHRNB1* (NM_009601.4; MIM #100710), *CHRND* (NM_021600.2; MIM #100720), and *CHRNE* (NM_000080.3; MIM #100725) encoding the AChR α, β, δ, and ε subunits, respectively.

Construction of Expression Vectors

Human $ACHE_T$, *COLQ* cDNAs, and LacZ were cloned and introduced into a cytomegalovirus-based mammalian expression vector pTargeT (Promega, Madison, WI) [Ohno et al., 1998]. Each mutation was introduced into *COLQ* cDNA using the QuikChange site-directed mutagenesis kit (Stratagene). The extracellular domain (aa 1–393) of human *MUSK* (NM_001166280.1; MIM #601296) cDNA (Open Biosystems/Thermo Scientific, Waltham, MA) was cloned into a mammalian expression vector pAPtag-5 (GenHunter, Nashville, TN) at the *Nbe*I and *Xbo*I sites upstream of a myc epitope [Kawakami et al., 2011].

Transfection and AChE Extraction

Wild-type or mutant pTargeT-*COLQ* was transfected into COS7 cells along with pTargeT-$ACHE_T$ in a 10-cm dish using X-tremeGENE 9 DNA Transfection Reagent (Roche Diagnostics, Indianapolis, IN). Cells were incubated at 37°C for 48 hr and scraped from dish in Tris–HCl buffer (50 mM Tris–HCl [pH 7.0], 0.5% Triton X-100, 0.2 mM EDTA, 2 μg/ml leupeptin, 1 μg/ml pepstatin, and 0.1 μmol/ml benzamidine) containing 1 M NaCl. The extract was vortexed in a 1.5-ml tube and centrifuged at 14,000*g* for 5 min, and the supernatant was obtained.

Sedimentation Analysis

A sedimentation analysis was performed as previously described [Ohno et al., 1998]. The AChE-containing supernatant was applied on a 5%–20% sucrose density gradient, which was made in Tris–HCl buffer along with β-galactosidase (16.1 S) and alkaline phosphatase (6.1 S) as internal sedimentation standards. Centrifugation was performed in a Beckman SW41Ti rotor at 4°C for 21 hr at 178300*g*. The collected fractions were assayed for AChE activities using the Ellman method [Ellman et al., 1961] and determined the absorbance at 420 nm using a Sunrise Absorbance Reader (Tecan, Männedorf, Switzerland).

Isolation of ColQ-Tailed AChE on a Heparin–Agarose Column

For isolation of ColQ-tailed AChE, the extract was diluted in Tris–HCl buffer containing 0.2 M NaCl and loaded onto a HiTrap Heparin HP column (GE Healthcare, Buckinghamshire, UK). We washed the column with five volumes of Tris–HCl buffer containing 0.2 M NaCl, and eluted ColQ-tailed AChE with Tris–HCl buffer containing 1 M NaCl. We concentrated the eluate with an Amicon Ultra-4 Centrifugal Filter (50K) (Millipore, Billerica, MA) [Kawakami et al., 2011; Kimbell et al., 2004].

Table 1. Clinical Features and Mutations

Pt.	Sex	Age	Onset	Walking	Noc. NIV	Edrophonium i.v.	RNS	rCMAP	Exon	Nucleotide change	Amino-acid change
1	M	19 y	Birth	19 m	12 y	No change	−52%	+	11	c.679C>T	p.Arg227X
									14	c.965T>A	p.Val322Asp
2	M	12 y	Birth	24 m	11 y	Respiratory distress	−32%	+	17	c.1339G>C[a]	p.Asp447His[a]
3	M	7 y	3 y	18 m	Not used	Improved	−79%	+	17	c.1331G>A	p.Cys444Tyr
									17	c.1354C>T	p.Arg452Cys

[a]Homozygous mutation.
Exon numbers are according to GenBank Accession NM_005677.3. Mutations are numbered according to NM_005677.3 (cDNA) and NP_005668.2 (protein). cDNA number +1 corresponds to the A of the ATG translation initiation codon.
Pt., patient; Noc. NIV, nocturnal noninvasive ventilation; RNS, repetitive nerve stimulation at 3 Hz of ulnar or accessory nerves; rCMAP, repetitive compound muscle action potential; m, months; y, years.

Transplantation of ColQ-tailed AChE to NMJs of *Colq*$^{-/-}$ Mice

We obtained approvals of the *Colq*$^{-/-}$ mice[Feng et al., 1999] studies by the Animal Care and Use Committee of the Nagoya University. We prepared 10-μm-thick sections of quadriceps muscles of *Colq*$^{-/-}$ mice with a Leica CW3050–4 cryostat at −20°C, and stored at −80°C until used. The muscle sections were fixed in acetone for 15 min. The stock solutions of ColQ-tailed AChE were diluted in Tris–HCl buffer containing 1 M NaCl and 5 mg/ml each of bovine serum albumin, chicken ovalbumin, and gelatin to give an Ellman unit equivalent to 1–2 ng of Torpedo AChE (Sigma, St. Louis, MO), and the NaCl concentration was adjusted to 0.5 M. To adjust the ionic strength of the solution, we added 50 mM Tris–HCl buffer stepwise over a period of 3 hr to 0.3 M NaCl. The slides were placed in a humidified chamber and incubated overnight at room temperature [Kimbell et al., 2004; Rotundo et al., 1997].

Immunofluorescence

For preparation of immunofluorescence, muscle sections were blocked with 5% horse serum in phosphate-buffered saline for 20 min. We detected ColQ-tailed AChE by anti-ColQ antibody [Ito et al., 2012] and anti rabbit-FITC secondary antibody at 1:100 (Vector Lab., Burlingame, CA), along with 2.5 μg/ml Alexa-594-conjugated α-bungarotoxin (Sigma) for visualizing AChR. Signals of ColQ and AChR were examined with fluorescent microscope, BX60 (Olympus, Tokyo, Japan). We analyzed more than 10 muscle sections for each experiment and representative images are indicated in the figures.

Preparation of the Extracellular Domain of MuSK

pAPtag-5 carrying hMuSKect-myc was transfected into HEK293 cells in a 10-cm dish using the calcium phosphate method. The hMuSKect-myc was purified with the c-myc-Tagged Protein Mild Purification Kit version 2 (MBL, Nagoya, Japan) [Kawakami et al., 2011].

In Vitro Plate-Binding assay for ColQ–MuSK Interaction

The Maxi-Sorp Immuno Plate (Nunc/Thermo Scientific) was coated with purified hMuSKect-myc at 4°C overnight and then blocked with phosphate-buffered saline containing 1% bovine serum albumin at room temperature for 1 hr. We incubated an equal Ellman unit of wild-type or mutant ColQ-tailed AChE at 4°C for 4 hr and then quantified the bound ColQ-tailed AChE by the Ellman method. Each time before we moved to the next step, we washed the plate three times with phosphate-buffered saline [Kawakami et al., 2011].

In Vivo Electroporation of pTarget-*COLQ*

The tibialis anterior muscles of *Colq*$^{-/-}$ mice were injected with 50 μg each of pTargeT-*COLQ* and pTargeT-LacZ plasmids. In vivo transfection was performed using an in vivo electroporator (CUY21EDIT; BEX Co., Ltd., Tokyo, Japan). A pair of electrode needles was inserted into the muscle in the longitudinal direction to a depth of 4 mm to encompass the plasmid-injected site. Pulses of 50 V and 25-msec were administered every 1 sec three times in forward polarity and three more times in the opposite polarity [Aihara and Miyazaki, 1998]. Seven days after the electroporation, mice were sacrificed and tibialis anterior muscles were analyzed.

AAV8-Mediated Expression of Mutant ColQ in *Colq*$^{-/-}$ Mice

We prepared wild-type and mutant pAAV8-*COLQ* and intravenously administered them to *Colq*$^{-/-}$ mice as described previously [Ito et al., 2012]. We inserted the wild-type human *COLQ* or mutant human *COLQ* harboring p.Asp447His into downstream of a CMV promoter in the pAAV-MCS vector using the AAV Helper-Free system (Stratagene). We employed AAV serotype 8 that can efficiently infect skeletal muscles. We injected 2×10^{12} vector genomes of wild-type or mutant pAAV-*COLQ* to the tail vein of 4-week-old male *Colq*$^{-/-}$ mice. Similar copies of wild-type pAAV8-*COLQ* and mutant pAAV8-*COLQ*-p.Asp447His genomes were transduced into muscle cells with a mean ratio of 1.07 (mutant transgene/wild-type transgene, $n = 3$). We quantified motor functions up to 4 weeks after injection. Muscle weakness and fatigability were measured with a rotarod apparatus (Ugo Basile). Mice were allowed to take a rest for 1 hr between each rotarod task and an average of three measurements was taken. Spontaneous running-wheel activities were used to quantify voluntary exercises. Each mouse was placed in a standard cage equipped with a counter-equipped running wheel (diameter, 14.7 cm; width, 5.2 cm; Ohara Medical Corp., Tokyo, Japan). The running distances were recorded every 24 hr. At 6 weeks after injection, mice were sacrificed and sections of skeletal muscles were stained for AChR and ColQ to visualize the transduced ColQ-tailed AChE as described above.

Results

Mutation Analysis

On the basis of combined clinical and electrophysiological features such as early age of onset, negative response to cholinesterase inhibitors, respiratory insufficiency, and repetitive muscle response [Abicht et al., 2012; Engel, 2012], we first sequenced *COLQ* and identified that each patient carried two mutant *COLQ* alleles. Patient 1 had heterozygous [c.679C>T, p.Arg227X] +

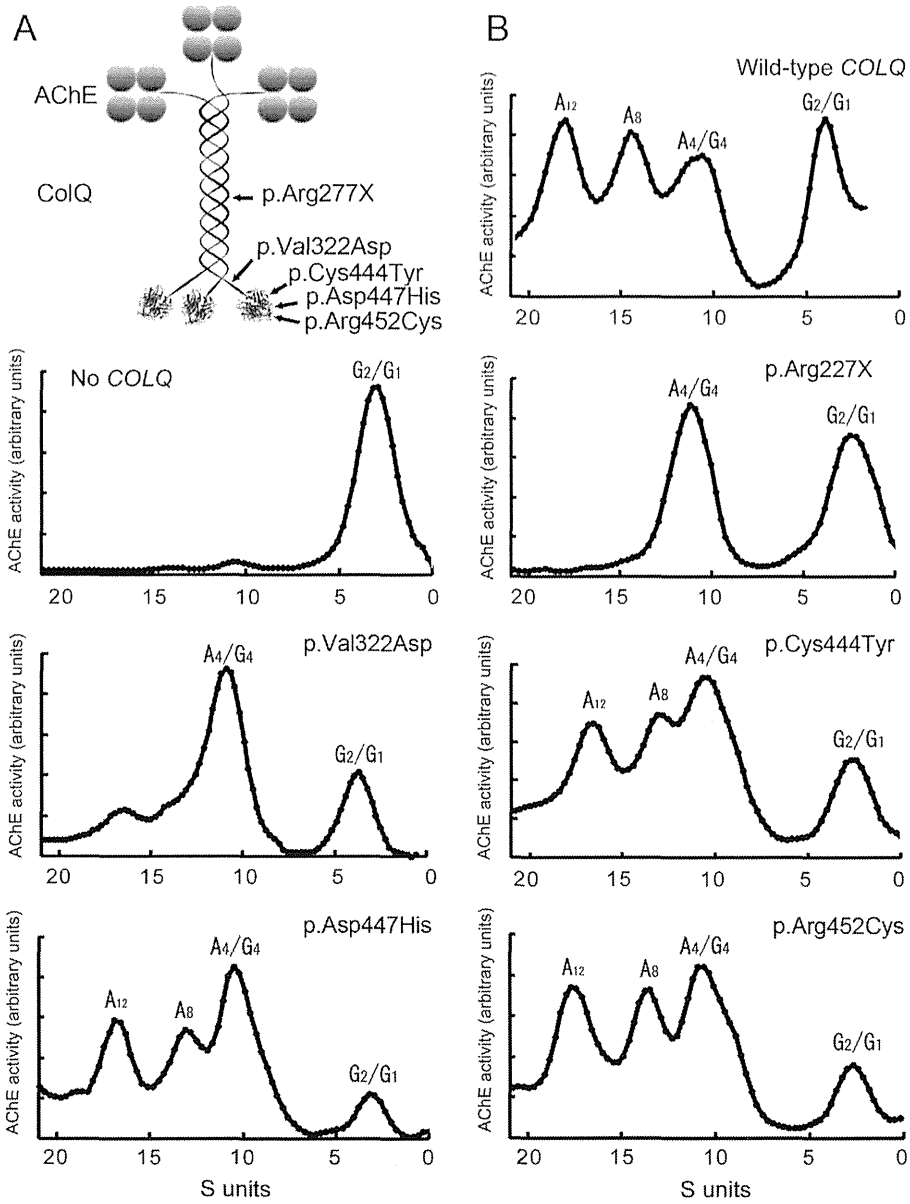

Figure 1. **A**: Schematic presentation of positions of the identified mutations in ColQ. **B**: Sedimentation profiles of AChE species extracted from COS cells transfected with wild-type *ACHE*$_T$ cDNA and indicated *COLQ* cDNA. p.Arg227X is in the collagen domain, the other four missense mutations are in the C-terminal domain. p.Val322Asp has a small ~16-S peak (A_{12} species), whereas the other missense mutations in the C-terminal region do not abolish formation of asymmetric AChE species. G_1, G_2, and G_4, globular forms; A_4, A_8, and A_{12}, asymmetric forms.

[c.965T>A, p.Val322Asp] mutations. Patient 2 was heterozygous for [c.1331G>A, p.Cys444Tyr] + [c.1354C>T, p.Arg452 Cys]. Patient 3 had a homozygous [c.1339G>C, p.Asp447His] mutation (Fig. 1A, Table 1, Supp. Fig. S1). We traced the mutations in the parents of patients 1 and 3, and found that the mutation on each allele was inherited from unaffected parents. In patient 2, we confirmed heterozygosity by cloning each allele of exon 17 and sequenced them. Among the five mutations, only c.1331G>A, p.Cys444Tyr was previously identified in another Japanese patient [Ohno et al., 2000], but its pathogenicity remained elusive [Kimbell et al., 2004]. The other four mutations were novel. All the amino acids at mutated codons were conserved across species [Ohno et al., 1998].

Sedimentation Profiles of Mutations

Four missense mutations were in CTD and the nonsense p.Arg227X was in the collagen domain. We first examined the effects of the mutations on formation of asymmetric ColQ-tailed AChE species in COS cells. The p.Arg227X mutation that truncates ColQ in its collagen domain did not produce normal A_{12} species of ColQ-tailed AChE, as has been observed in other truncation mutations in the collagen domain [Ohno et al., 1998; 2000]. The p.Val322Asp mutation close to the N-terminal end of CTD similarly failed to produce A_{12} species. By contrast, the other three CTD mutations (p.Cys444Tyr, p.Asp447His, and p.Arg452Cys) produced

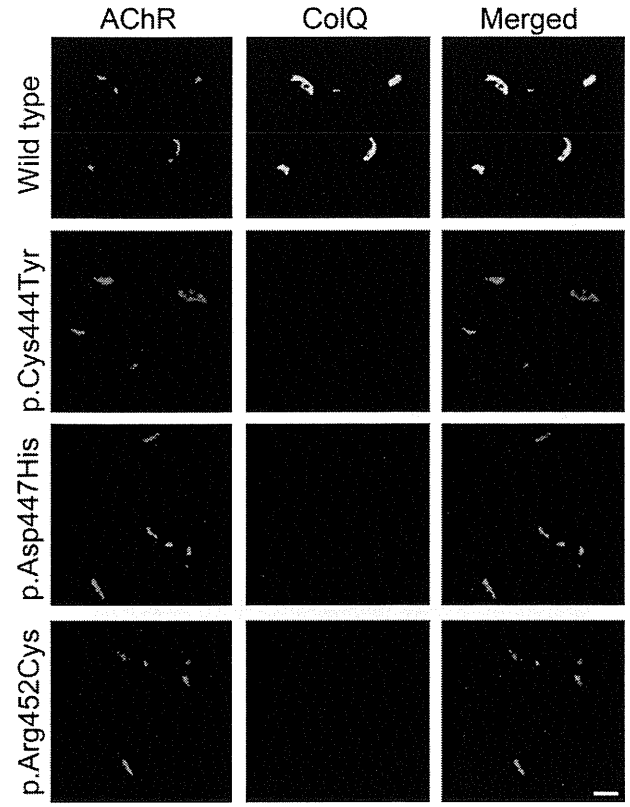

Figure 2. In vitro overlay assays. Plasmid encoding the indicated CTD mutations of human ColQ were cotransfected into COS cells together with a plasmid encoding the wild-type human $AChE_T$ catalytic subunit. The A_{12} AChE expressed in COS cells was isolated and overlaid on a 10-μm quadriceps muscle section of *Colq*$^{-/-}$ mice. ColQ-tailed AChE molecules harboring the indicated mutations do not colocalize with AChRs. ColQ is stained with anti-ColQ antibody and AChR with Alexa594-labeled α-bungarotoxin. Scale bar = 20 μm.

normal or slightly reduced peaks of asymmetric A_4, A_8, and A_{12} species compared to the wild-type (Fig. 1B).

Overlay of CTD Mutants to the NMJ of *Colq*$^{-/-}$ Mice

We overlaid the purified recombinant human ColQ-tailed AChE protein complex on a section of skeletal muscle of *Colq*$^{-/-}$ mice. Wild-type ColQ-tailed AChE colocalized with AChR at the NMJs, whereas ColQ-tailed AChE with p.Cys444Tyr, p.Asp447His, and p.Arg452Cys mutations failed to colocalize with AChR (Fig. 2). This assay showed that these CTD mutations impair anchoring of ColQ at the vertebrate NMJs.

In Vitro Plate-Binding Assay for ColQ–MuSK Interaction

As the synaptic anchorage of AChE by ColQ is partly dependent on the association of ColQ with MuSK [Cartaud et al., 2004], we next examined whether the CTD mutations had an effect on the interaction of human ColQ and human MuSK using an in vitro plate-binding assay. We coated the plate with purified hMuSKect-myc, and added a fixed amount of the purified recombinant human ColQ-tailed AChE protein complex. The bound AChE was quantified by the Ellman method. AChE activities of the CTD mutants carrying p.Cys444Tyr, p.Asp447His, and p.Arg452Cys were significantly lower than that of wild-type CTD (Fig. 3). These results showed that impaired anchoring of the mutant ColQ-tailed AChE was due to the lack of interaction between ColQ and MuSK.

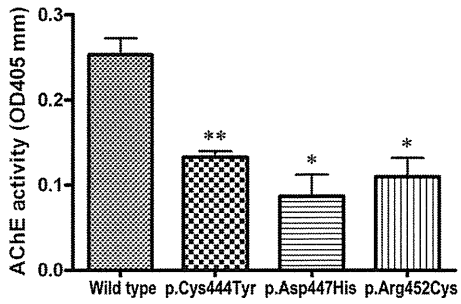

Figure 3. In vitro plate-binding assays. The extracellular domain of human MuSK (hMuSKect-myc) was coated on a 96-well plate. Purified recombinant ColQ-tailed AChE was overlaid on the plate. Bound ColQ-tailed AChE was quantified by AChE activity. $^*P < 0.05$, $^{**}P < 0.01$ by Student's *t*-test.

In Vivo Electroporation of *COLQ* with CTD Mutations into the Muscles of *Colq*$^{-/-}$ Mice

To confirm whether the three CTD mutants indeed impair anchoring of ColQ-tailed AChE to the NMJ in vivo, we electroporated wild-type and mutant pTargeT-*COLQ* constructs to tibialis anterior muscles of *Colq*$^{-/-}$ mice. We first confirmed that the pTargeT-LacZ plasmid is efficiently transduced into muscle fibers (Fig. 4A). ColQ-tailed AChE harboring p.Cys444Tyr, p.Asp447His, and p.Arg452Cys in CTD did not anchor to the NMJs of *Colq*$^{-/-}$ mice (Fig. 4), although real-time RT-PCR revealed similar expression levels of the wild-type and mutant *COLQ* mRNAs (ranges of *COLQ*/*Gapdh* mRNAs = 0.03 to 0.11 for wild-type and three mutants). These studies revealed that the three mutant ColQ molecules were incompetent for anchoring to the NMJ in vivo.

AAV8-Mediated Expression of Mutant ColQ in *Colq*$^{-/-}$ Mice

We previously reported the protein-anchoring therapy for *Colq*$^{-/-}$ mice, in which ColQ-tailed AChE is moved to and anchored to remote NMJs using its proprietary binding affinities for perlecan and MuSK [Ito et al., 2012]. To directly prove that the CTD mutations compromise anchoring of ColQ to the NMJ in a model animal, we intravenously administered wild-type and p.Asp447His-mutant AAV8-*COLQ* to *Colq*$^{-/-}$ mice, and analyzed motor functions and histological localization of ColQ. Motor functions evaluated by the dwell time on a rotarod (Fig. 5A) and by voluntary movements (Fig. 5B) were prominently improved in *Colq*$^{-/-}$ mice treated with wild-type *COLQ* but not with p.Asp447His-*COLQ*. Histological studies similarly showed that ColQ was colocalized to AChR in *Colq*$^{-/-}$ mice treated with AAV-wild-type *COLQ* but not with AAV-p.Asp447His-*COLQ* (Fig. 5C).

Discussion

CMSs have a variety of causes that lead to defects in the NMJ signal transmission. Elucidation of the molecular pathomechanisms is essential to develop and provide a specific treatment for CMS patients. Ephedrine and albuterol are effective for patients with

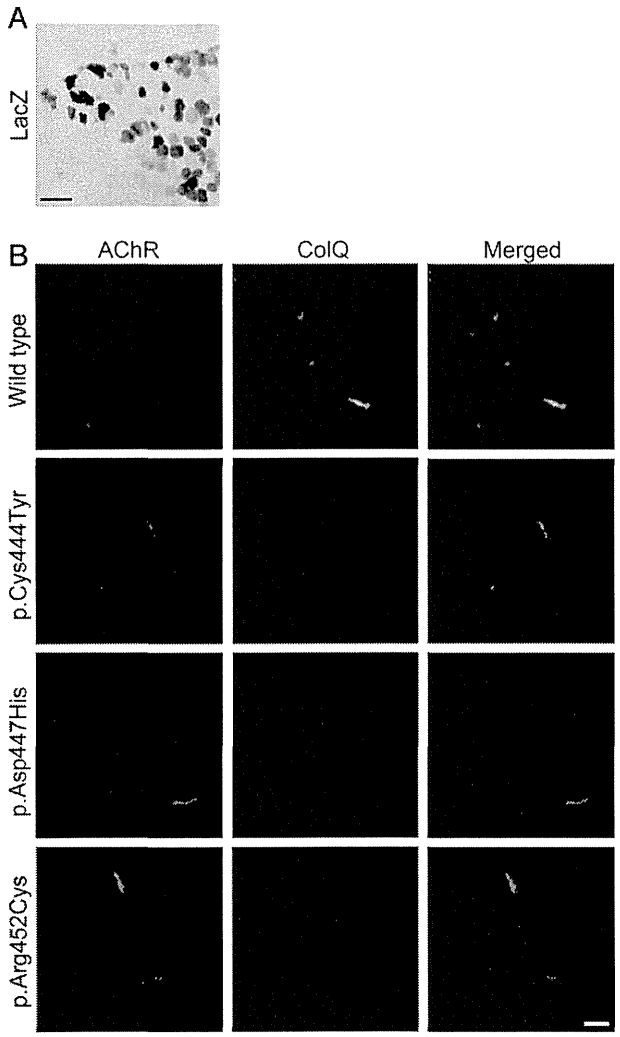

Figure 4. In vivo electroporation. **A**: Histochemical staining for β-galactosidase activity in the muscle after gene transfer of pTargeT-lacZ with electroporation. The transverse section of the muscle was stained with X-gal. **B**: Immunocytochemistry using serial muscle sections showed that ColQ-tailed AChE molecules harboring p.Val322Asp, p.Asp447His, p.Cys444Tyr, and p.Arg452Cys in ColQ, do not colocalize with AChRs in tibialis anterior muscles of *Colq*$^{-/-}$ mice. ColQ is stained with anti-ColQ antibody and AChR with Alexa594-labeled α-bungarotoxin. Scale bar = 100 μm (**A**) and 20 μm (**B**).

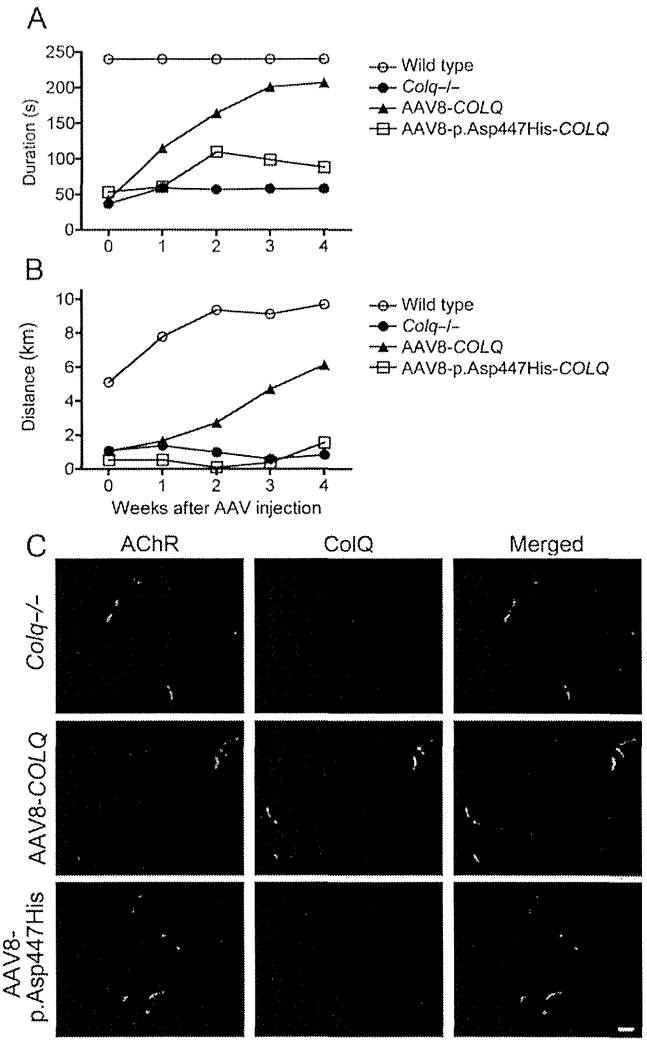

Figure 5. AAV8-mediated expression of mutant ColQ in *Colq*$^{-/-}$ mice. **A**: Temporal profiles of dwell times on a rotarod that linearly accelerated from 0 to 40 rpm in 240 sec. **B**: Voluntary movements per day were quantified with a counter-equipped running wheel. **C**: Visualization of ColQ-AChE and AChR on the section of skeletal muscle using anti-ColQ antibody and α-bungarotoxin, respectively. AAV8-*COLQ*-p.Asp447His failed to anchor ColQ-tailed AChE to the NMJ. Scale bar = 20 μm.

endplate AChE deficiency harboring *COLQ* mutations [Chan et al., 2012; Engel et al., 2010]. Cholinesterase inhibitors cannot improve neuromuscular transmission and often worsen myasthenic symptoms and respiratory conditions. Therefore, an early genetic diagnosis is important for the patients. Clinical features of the three patients prompted us to search for mutations in *COLQ*, and indeed we detected five *COLQ* mutations. Four of them are novel and p.Cys444Tyr has been previously reported in another Japanese patient [Ohno et al., 2000]. It is interesting to note that the five mutations are unique to Japanese patients, which suggests that all the mutations have recently arisen in the patients' families and are unlikely to be founder mutations.

In 1998, we cloned human *COLQ* cDNA, identified its genomic structure, and detected *COLQ* mutations in patients with endplate AChE deficiency [Ohno et al., 1998]. We also proved that mutations in the collagen domain impair formation of ColQ-tailed AChE [Ohno et al., 1998]. We later reported four classes of *COLQ* mutations as stated in the introduction, and proved pathogenicity in three classes but not in a class comprising CTD mutations [Ohno et al., 1999; 2000]. We next proved pathogenicity of five mutations (p.Arg315X, p.Asp342Glu, p.Gln371X, p.Arg410Gln, and p.Arg410Pro) in CTD using the heterologous overlay of human ColQ-tailed AChE to the frog muscles, but another mutation, p.Cys444Tyr, had no effect on anchoring of ColQ to the frog NMJ [Kimbell et al., 2004]. To summarize, we have reported 23 *COLQ* mutations and have succeeded in proving the pathogenicity in 22 mutations [Kimbell et al., 2004; Ohno et al., 1998; 1999; 2000; Shapira et al., 2002]. p.Cys444Tyr in CTD has thus been the only mutation that we failed to prove why the patient was deficient for AChE. Donger et al. (1998) reported p.Tyr430Ser in CTD in a patient with endplate AChE deficiency, but the sedimentation analysis yielded normal asymmetric species of AChE. The p.Tyr430Ser mutation was later employed to prove that CTD binds to MuSK by immunoprecipitation experiments [Cartaud et al., 2004]. Four

additional mutations (p.Arg341Gly, p.Cys386Ser, p.Cys417Tyr, and p.Thr441Ala) in CTD have been reported by others but none have been functionally analyzed [Mihaylova et al., 2008; Muller et al., 2004].

In the present study, we found four missense mutations (p.Val322Asp, p.Asp447His, p.Cys444Tyr, and p.Arg452Cys) in CTD and one truncation mutation (p.Arg227X) in the collagen domain in three patients with endplate AChE deficiency. Three mutations (p.Val322Asp, p.Asp447His, and p.Arg452Cys) in CTD have not been functionally characterized and one was p.Cys444Tyr, for which the pathogenicity remained elusive. We characterized the functional consequences of these mutations.

The analysis of sedimentation profiles revealed that p.Arg227X and p.Val322Asp abolish formation of normal asymmetric A_{12} species of AChE. p.Val322Asp is the only mutation that affects formation of A_{12} and is the only mutation that introduces a negatively charged residue in CTD. We previously reported that 1082delC in CTD introduces 64 hydrophobic missense residues after the frameshift, which prevents triple helix formation [Ohno et al., 2000]. CTD is enriched with prolines, cysteines, and charged residues. The hydrophobicity profile is likely to be essential in CTD. p.Val322Asp introduces a hydrophilic aspartate residue, and disrupts a hydrophobic cluster close to the N-terminal end of CTD (Supp. Fig. S2A). Prediction of a secondary structure similarly demonstrates shortening of a β-sheet and de novo insertion of a turn before an α-helix (Supp. Fig. S2B). We do not observe these gross alterations in predicted structures with p.Cys444Tyr, p.Asp447His, and p.Arg452Cys (Supp. Fig. S2). p.Val322Asp is thus likely to compromise the tertiary structure of CTD and leads to defective triple helix formation.

The analysis of sedimentation profiles showed that the other CTD mutations, p.Cys444Tyr, p.Asp447His, and p.Arg452Cys, generated normal asymmetric A_{12} species of AChE. We next examined the anchoring competence of these mutations. We had previously employed frog muscles to analyze anchoring incompetence of CTD mutations, but failed to prove it for p.Cys444Tyr [Kimbell et al., 2004]. We thus used the vertebrate NMJs of *Colq*$^{-/-}$ mice, and proved that all three mutations are not able to anchor to the mouse NMJ. Anchoring competence of p.Cys444Tyr to frog NMJs but not to mouse NMJs suggests that p.Cys444Tyr does not grossly change the conformation of CTD and is likely to be a mild mutation. Indeed, the onset of patient 3 carrying p.Cys444Tyr was at the age of 3 years, and the patient started walking at 18 months, which are the mildest among the three currently analyzed patients.

To further dissect the underlying molecular bases of anchoring incompetence of p.Cys444Tyr, p.Asp447His, and p.Arg452Cys, we quantified the ColQ–MuSK interaction by the in vitro plate-binding assay, which enabled us to estimate the binding affinities of these two molecules. The three missense mutations decreased the activities of ColQ-tailed AChE bound to MuSK to ~50% or less, which suggests that ~50% reduction of the binding affinity is likely to be required to compromise anchoring of ColQ to the NMJ.

Moreover, we demonstrated the pathogenicity of the mutations in a model animal for the first time. We electroporated the three CTD mutations into tibialis anterior muscles of *Colq*$^{-/-}$ mice, and found that each mutation was indeed anchoring-incompetent. To further prove the pathogenicity of one of the mutations in *Colq*$^{-/-}$ mice, we intravenously injected AAV8-*COLQ*-p.Asp447His to *Colq*$^{-/-}$ mice and found that motor deficits remained essentially the same and anchoring of ColQ was not observed at the NMJs.

In vitro plate-binding assays revealed ~50% reduction of binding affinity of ColQ for MuSK for p.Cys444Tyr, p.Asp447His, and p.Arg452Cys (Fig. 3), but these mutants were not at all anchored to the NMJ by in vitro overlay assay (Fig. 2), in vivo electroporation (Fig. 4), and AAV8 treatment (Fig. 5). Among the three mutants, p.Cys444Tyr showed the most preserved binding affinity for MuSK, which, however, was not sufficient to anchor the mutant ColQ to the NMJ in in vitro overlay assay (Fig. 2) and in vivo electroporation (Fig. 4). The presence of heparan sulfate proteoglycans like perlecan at the NMJ in these assays was unlikely to sufficiently compensate for the defective CTD-MuSK interaction, which also underscores a pivotal role of CTD-MuSK interaction on binding of ColQ to the NMJ. Although the same amount of ColQ-tailed AChE was used for in vitro plate-binding and in vitro overlay assays, the amount of MuSK (>150 ng/well) used in in vitro plate-binding assay was likely to be much more than that at the NMJ in in vitro overlay assay, which may account for the difference in up to 50% preservation of ColQ binding in in vitro plate-binding assay and complete lack of ColQ binding in in vitro overlay assay.

Acknowledgments

We thank Yasutaka Ohya, Kumiko Yano, and Koji Nomaru at Division for Research of Laboratory Animals of Nagoya University for technical assistance.

Disclosure statement: The authors declare no conflict of interest.

References

Abicht A, Dusl M, Gallenmuller C, Guergueltcheva V, Schara U, Della Marina A, Wibbeler E, Almaras S, Mihaylova V, von der Hagen M, Huebner A, Chaouch A, et al. 2012. Congenital myasthenic syndromes: achievements and limitations of phenotype-guided gene-after-gene sequencing in diagnostic practice: a study of 680 patients. Hum Mutat 33:1474–1484.

Aihara H, Miyazaki J. 1998. Gene transfer into muscle by electroporation in vivo. Nat Biotechnol 16:867–870.

Arikawa-Hirasawa E, Rossi SG, Rotundo RL, Yamada Y. 2002. Absence of acetylcholinesterase at the neuromuscular junctions of perlecan-null mice. Nat Neurosci 5:119–123.

Cartaud A, Strochlic L, Guerra M, Blanchard B, Lambergeon M, Krejci E, Cartaud J, Legay C. 2004. MuSK is required for anchoring acetylcholinesterase at the neuromuscular junction. J Cell Biol 165:505–515.

Chan SH, Wong VC, Engel AG. 2012. Neuromuscular junction acetylcholinesterase deficiency responsive to albuterol. Pediatr Neurol 47:137–140.

Donger C, Krejci E, Pou Serradell A, Eymard B, Bon S, Nicole S, Chateau D, Gary F, Fardeau M, J. M, Guicheney P. 1998. Mutation in the human acetylcholinesterase-associated collagen gene, *COLQ*, is responsible for congenital myasthenic syndrome with end-plate acetylcholinesterase deficiency (Type Ic). Am J Hum Genet 63:967–975.

Ellman GL, Courtney KD, Andres V, Jr., Feather-Stone RM. 1961. A new and rapid colorimetric determination of acetylcholinesterase activity. Biochem Pharmacol 7:88–95.

Engel AG. 2012. Congenital myasthenic syndromes in 2012. Curr Neurol Neurosci Rep 12:92–101.

Engel AG, Lambert EH, Gomez MR. 1977. A new myasthenic syndrome with end-plate acetylcholinesterase deficiency, small nerve terminals, and reduced acetylcholine release. Ann Neurol 1:315–330.

Engel AG, Ohno K, Sine SM. 2003. Sleuthing molecular targets for neurological diseases at the neuromuscular junction. Nat Rev Neurosci 4:339–352.

Engel AG, Shen XM, Selcen D, Sine SM. 2010. What have we learned from the congenital myasthenic syndromes. J Mol Neurosci 40:143–153.

Feng G, Krejci E, Molgo J, Cunningham JM, Massoulie J, Sanes JR. 1999. Genetic analysis of collagen Q: roles in acetylcholinesterase and butyrylcholinesterase assembly and in synaptic structure and function. J Cell Biol 144:1349–1360.

Ito M, Suzuki Y, Okada T, Fukudome T, Yoshimura T, Masuda A, Takeda S, Krejci E, Ohno K. 2012. Protein-anchoring strategy for delivering acetylcholinesterase to the neuromuscular junction. Mol Ther 20:1384–1392.

Kawakami Y, Ito M, Hirayama M, Sahashi K, Ohkawara B, Masuda A, Nishida H, Mabuchi N, Engel AG, Ohno K. 2011. Anti-MuSK autoantibodies block binding of collagen Q to MuSK. Neurology 77:1819–1826.

Kimbell LM, Ohno K, Engel AG, Rotundo RL. 2004. C-terminal and heparin-binding domains of collagenic tail subunit are both essential for anchoring acetylcholinesterase at the synapse. J Biol Chem 279:10997–11005.

Massoulie J. 2002. The origin of the molecular diversity and functional anchoring of cholinesterases. Neurosignals 11:130–143.

Mihaylova V, Muller JS, Vilchez JJ, Salih MA, Kabiraj MM, D'Amico A, Bertini E, Wolfle J, Schreiner F, Kurlemann G, Rasic VM, Siskova D, et al. 2008. Clinical and molecular genetic findings in COLQ-mutant congenital myasthenic syndromes. Brain 131:747–759.

Muller JS, Petrova S, Kiefer R, Stucka R, Konig C, Baumeister SK, Huebner A, Lochmuller H, Abicht A. 2004. Synaptic congenital myasthenic syndrome in three patients due to a novel missense mutation (T441A) of the COLQ gene. Neuropediatrics 35:183–189.

Ohno K, Brengman J, Tsujino A, Engel AG. 1998. Human endplate acetylcholinesterase deficiency caused by mutations in the collagen-like tail subunit (ColQ) of the asymmetric enzyme. Proc Natl Acad Sci USA 95:9654–9659.

Ohno K, Brengman JM, Felice KJ, Cornblath DR, Engel AG. 1999. Congenital endplate acetylcholinesterase deficiency caused by a nonsense mutation and an A–>G splice-donor-site mutation at position +3 of the collagenlike-tail-subunit gene (COLQ): how does G at position +3 result in aberrant splicing? Am J Hum Genet 65:635–644.

Ohno K, Engel AG, Brengman JM, Shen X-M, Heidenrich FR, Vincent A, Milone M, Tan E, Demirci M, Walsh P, Nakano S, Akiguchi I. 2000. The spectrum of mutations causing endplate acetylcholinesterase deficiency. Ann Neurol 47:162–170.

Rotundo RL, Rossi SG, Anglister L. 1997. Transplantation of quail collagen-tailed acetylcholinesterase molecules onto the frog neuromuscular synapse. J Cell Biol 136:367–374.

Shapira YA, Sadeh ME, Bergtraum MP, Tsujino A, Ohno K, Shen XM, Brengman J, Edwardson S, Matoth I, Engel AG. 2002. Three novel COLQ mutations and variation of phenotypic expressivity due to G240X. Neurology 58:603–609.

Sigoillot SM, Bourgeois F, Lambergeon M, Strochlic L, Legay C. 2010. ColQ controls postsynaptic differentiation at the neuromuscular junction. J Neurosci 30:13–23.

ORPHANET JOURNAL OF RARE DISEASES

RESEARCH Open Access

Perhexiline maleate in the treatment of fibrodysplasia ossificans progressiva: an open-labeled clinical trial

Hiroshi Kitoh[1*], Masataka Achiwa[2], Hiroshi Kaneko[1], Kenichi Mishima[1], Masaki Matsushita[1], Izumi Kadono[3], John D Horowitz[4], Benedetta C Sallustio[4], Kinji Ohno[5] and Naoki Ishiguro[1]

Abstract

Background: Currently, there are no effective medical treatment options to prevent the formation of heterotopic bones in fibrodysplasia ossificans progressiva (FOP). By the drug repositioning strategy, we confirmed that perhexiline maleate (Pex) potentially ameliorates heterotopic ossification in model cells and mice. Here, we conducted a prospective study to assess the efficacy and safety of Pex in the treatment of FOP patients.

Methods: FOP patients in this open-label single-center study were treated with Pex for a total of 12 months, and followed up for 12 consecutive months after medication discontinuation. The safety of the treatment was assessed regularly by physical and blood examinations. The efficacy of Pex for preventing heterotopic ossifications was evaluated by the presence of flare-ups, measurements of serum bone markers, and changes in the total bone volume calculated by the three-dimensional computed tomography (3D-CT) images.

Results: Five patients with an average age of 23.4 years were enrolled. Within safe doses of Pex administration in each individual, there were no drug-induced adverse effects during the medication phase. Three patients showed no intense inflammatory reactions during the study period, while two patients had acute flare-ups around the hip joint without evidence of trauma during the medication phase. In addition, one of them became progressively incapable of opening her mouth over the discontinuation phase. Serum levels of alkaline phosphatase (ALP) and bone specific ALP (BAP) were significantly and synchronously increased with the occurrence of flare-ups. Volumetric 3D-CT analysis demonstrated a significant increase in the total bone volume of Case 2 (378 cm^3) and Case 3 (833 cm^3) during the two-year study period.

Conclusions: We could not prove the efficacy of oral Pex administration in the prevention of heterotopic ossifications in FOP. Serum levels of ALP and BAP appear to be promising biomarkers for monitoring the development of ectopic ossifications and efficacy of the therapy. Quantification of change in the total bone volume by whole body CT scanning could be a reliable evaluation tool for disease progression in forthcoming clinical trials of FOP.

Keywords: Fibrodysplasia ossificans progressiva, Perhexiline maleate, Clinical trial, Biomarker, Whole body CT

Background

Fibrodysplasia ossificans progressiva (FOP) (OMIM: 135100) is a severely disabling heritable disorder of connective tissue characterized by congenital malformations of the great toes and progressive heterotopic ossification in various extraskeletal sites. FOP is very rare with a worldwide prevalence of approximately 1/2,000,000 [1]. It is caused by a recurrent activating mutation (617G > A, R206H) in the gene encoding activin A receptor type I (*ACVR1*)/activin-like kinase 2 (*ALK2*), a bone morphogenetic protein (BMP) type I receptor [2]. In FOP, the mutant receptor causes up-regulation of a transcriptional factor, *Id1*. Typically, during the first decade of life, sporadic episodes of painful soft tissue swellings (flare-ups) occur, which can transform skeletal muscles, tendons, ligaments, fascia, and aponeuroses

* Correspondence: hkitoh@med.nagoya-u.ac.jp
[1]Department of Orthopaedic Surgery, Nagoya University Graduate School of Medicine, 65 Tsurumai, Showa-ku, Nagoya, Aichi 466-8550, Japan
Full list of author information is available at the end of the article

into heterotopic bone [3]. Progressive heterotopic ossifications span the joints, lock them in place, and render movement impossible [4]. Immobility is cumulative and most patients are wheelchair-bound by the end of second decade of life [5]. Attempts to remove heterotopic bones usually lead to explosive new bone formation.

At present, there is no definitive pharmacotherapy to prevent progressive heterotopic ossifications in FOP. Recently, dorsomorphin and LDN-193189, a selective inhibitor of BMP type I receptor kinases, have been reported to inhibit activation of the BMP signaling in cultures cells and mice [6,7]. Similarly, CD1530, an agonist of nuclear retinoic acid receptor-γ, prevented heterotopic ossification in FOP model mice [8]. None of these compounds, however, has been applied in clinical practice.

A promising alternative for orphan diseases is the drug repositioning strategy, in which a drug currently used for patients with a specific disease is applied to another disease [9]. The advantage of this strategy is that the identified drugs are readily available and the adverse effects are known. In order to search for clinically applicable drugs for FOP, we screened 1040 FDA-approved drugs for suppression of the *Id1* promoter activated by the mutant *ACVR1/ALK2* in mouse C2C12 myoblasts. We found that perhexiline maleate (Pex), which is a prophylactic antianginal drug widely used for stable angina but its use markedly declined in the early 1980s after reports of hepatotoxicity and peripheral neuropathy, suppressed the *Id1* promoter activity and mRNA expression of native *Id1* and alkaline phosphatase by down-regulating phosphorylation of Smad1/5/8. Pex also reduced the volume of heterotopic ossification in crude BMP-induced model mice [10]. Here, we conducted an open-labeled clinical trial of Pex administration in the management of FOP.

Methods

This study was a non-randomized, non-placebo-controlled investigation to prospectively estimate the effect of Pex treatment in FOP patients. Eligible for participation were the patients who presented classic features of FOP including congenital malformation of the great toes and progressive heterotopic ossification of soft tissues, and those who had R206H mutation in the *ACVR1/ALK2* gene [11]. Because safety of Pex administration in children has not been established, skeletally immature patients were excluded from the study. Since there is no known effective treatment in preventing heterotopic ossification of FOP, we did not exclude the patients who received concurrent use of other medications, such as nonsteroidal anti-inflammatory drugs (NSAIDs) or cyclooxygenase-2 (COX-2) inhibitors. After approval from the Institutional Review Boards of the Nagoya University, patients who provided written informed consent were enrolled in the study.

All patients continued to receive Pex administration for a total of 12 months. At the end of this period, they discontinued Pex pharmacotherapy and were monitored for 12 consecutive months of discontinuation follow-up phase. After two weeks administration of an initial dose of 100 mg/day, plasma concentration of Pex was measured to adjust the dosage in each individual. Therapeutic drug monitoring was then regularly performed during the medication phase by Drs. John D. Horowitz and Benedetta C. Sallustio (Queen Elizabeth Hospital, Woodville, Australia), and an optimal dose of oral Pex administration was individually determined based on a range for Pex of 0.15-0.60 mg/L. The Safety of treatment was assessed by a monthly physical examination and a complete blood count/serum chemistry evaluation every three months, with a special care for known adverse effects of Pex including peripheral neuropathy and drug induced hepatic dysfunction [12]. The efficacy of Pex for preventing heterotopic ossifications was evaluated clinically and biochemically, as well as by volumetric computed tomography (CT). Careful physical examination was performed on each patient to observe the presence of flare-ups and the development of new ectopic ossifications. Serum concentrations of non-specific alkaline phosphatase (ALP), bone-specific alkaline phosphatase (BAP) and osteocalcin (OC) were measured at baseline, after 1, 3, 6, 9, and 12 months of Pex treatment (M: medication phase), and after 1, 3, 6, 9, and 12 months of medication discontinuation (D: discontinuation phase), using the commercially available Japan Society of Clinical Chemistry (JSCC) method, enzyme immunoassay (EIA), and radioimmunoassay (RIA) respectively (SRL Inc, Japan). For quantitative evaluation of ectopic bones to be formed, whole body scanning by 16 slice multi-detector CT was performed before the intervention (baseline), at the end of Pex medication (M-12 m: 12 months after commencement of treatment), and at the end of the study (D-12 m: 12 months after medication discontinuation). Due to various degrees of contractures in the upper and lower extremities as well as in the trunk, the top of the skull or periphery of the limbs sometimes failed to be imaged in some patients. Thus, we defined structural regions of interest (ROI) as the maximum 3D-CT imaging ranges to be analyzable which was standardized in each individual. Based on 3D-CT images, total bone volume (expressed as cm^3) in each patient was calculated by quantitative density analysis. The volume of newly formed bones was quantified by change in the total bone volume during the medication and discontinuation phases.

Table 1 Patients' characteristics and clinical outcome

Case	Age (years)	Gender	Dose of Pex	Adverse events	Acute inflammatory reaction (site)
1	36	Male	150 mg/d	None	None
2	26	Male	200 mg/d	None	M-7 m (right proximal thigh)
3	18	Female	75 mg/d	None	M-8 m (left hip), D-2 m (right jaw)
4	18	Female	14 mg/d	None	None
5	19	Male	100 mg/d	None	None

Pex = Perhexiline maleate; M-7 m = Medication phase at 7 months.
M-8 m = Medication phase at 8 months;
D-2 m = Discontinuation phase at 2 months.

Result

Five FOP patients were enrolled in the study between July 2010 and July 2012 (Table 1). There were three males and two females with an average age of 23.4 years (range, 18–36 years). All patients had significant deformities associated with severely restricted mobility of the spine and limbs. Two patients were confined to a wheelchair and required assistance in performing activities of daily living. Two patients received concurrent treatment with COX-2 inhibitor on a regular basis, and three patients irregularly took fast-acting NSAIDs when they felt pain. Under strictly controlling plasma concentration of Pex within 0.15-0.60 mg/L, the steady dosage of Pex varied between individuals from 14 mg/day (100 mg/week) to 200 mg/day. No obvious drug-induced adverse effects were found and no patients discontinued Pex administration during the whole period of treatment.

In three of the five patients, there were no intense inflammatory reactions associated with flare-ups during the study period, although this could happen randomly (Table 1). On the other hand, acute flare-ups were observed in two patients (Cases 2 and 3) without evidence of trauma during the medication phase (M-7 m and M-8 m, respectively) and high-dose corticosteroid treatment was administered in each patient at the beginning of flare-ups according to the treatment guidelines of International Fibrodysplasia Ossificans Progressiva Association (IFOPA) [13]. These flare-ups occurred in the right proximal thigh in Case 2 and

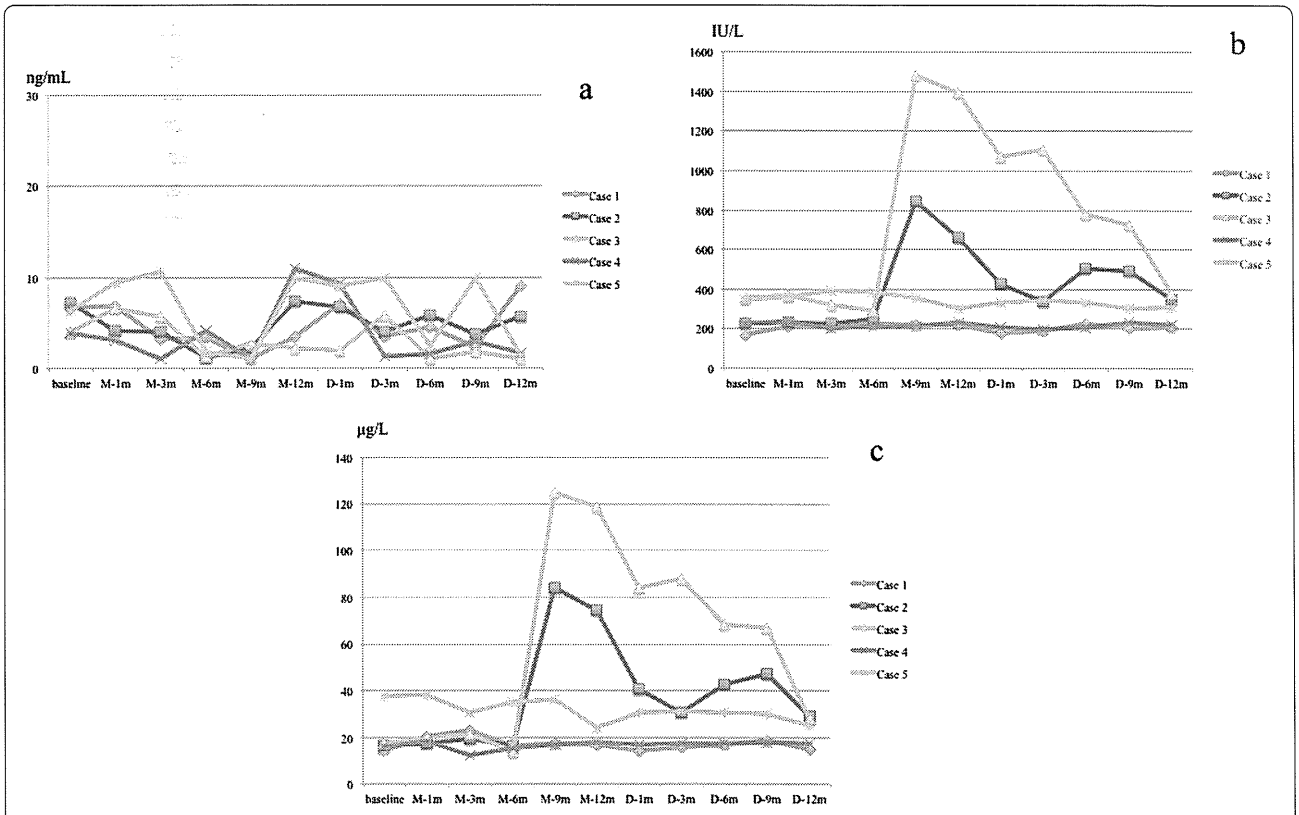

Figure 1 Serial measurements of serum osteocalcin (a), alkaline phosphatase (ALP) (b) and bone-specific alkaline phosphatase (BAP) (c) from 5 FOP patients. Serum levels of osteocalcin were maintained within the normal range during the study period in all patients. Serum levels of ALP rapidly elevated at M-9 m in Cases 2 and 3 who showed acute flare-ups at M-7 m and M-8 m, respectively. Case 3, who showed acute inflammation of her right jaw at D-2 m, had persistent higher ALP levels at D-3 m. Changes in serum BAP activity positively correlated to those in serum ALP levels.

around the left hip joint in Case 3. Following flare-ups, their hip joint mobility gradually deteriorated. In addition, Case 3 complained of severe right jaw pain and subsequent difficulty in mouth opening during the early discontinuation phase (D-2 m). Limited opening of the mouth resulted in interference with eating and oral hygiene.

Serum concentration of OC had no significant change in all patients (Figure 1a). During the whole study period, serum ALP and BAP levels were maintained at a normal range in the three patients who did not have inflammatory reactions. In the other two patients (Cases 2 and 3), on the other hand, these bone markers significantly and synchronously elevated following the occurrence of flare-ups during medication phase (Figure 1b,c). Elevated ALP and BAP levels were gradually reduced with time, but in Case 3, both bone markers rebounded with acute inflammation of her right jaw during the early discontinuation phase.

Quantitative 3D-CT analysis demonstrated that the total bone volume did not change in three patients (Cases 1, 4, and 5) during the study period, while a substantial increase in the total bone volume, both during the medication and discontinuation phases, was found in two patients (Figure 2a,b). In Case 2, increased bone volume of 223 cm^3 during the medication phase and that of 155 cm^3 during the discontinuation phase seemed to be associated with heterotopic bone formations in the right adductor muscle, and around the mid-femur, respectively (Figure 3a-g). In Case 3, there was an increase of 297 cm^3 in the total bone volume during the medication phase, which seemed to be related to intramuscular ossification in her left iliopsoas (Figure 4a-d). She also showed a maximal increased

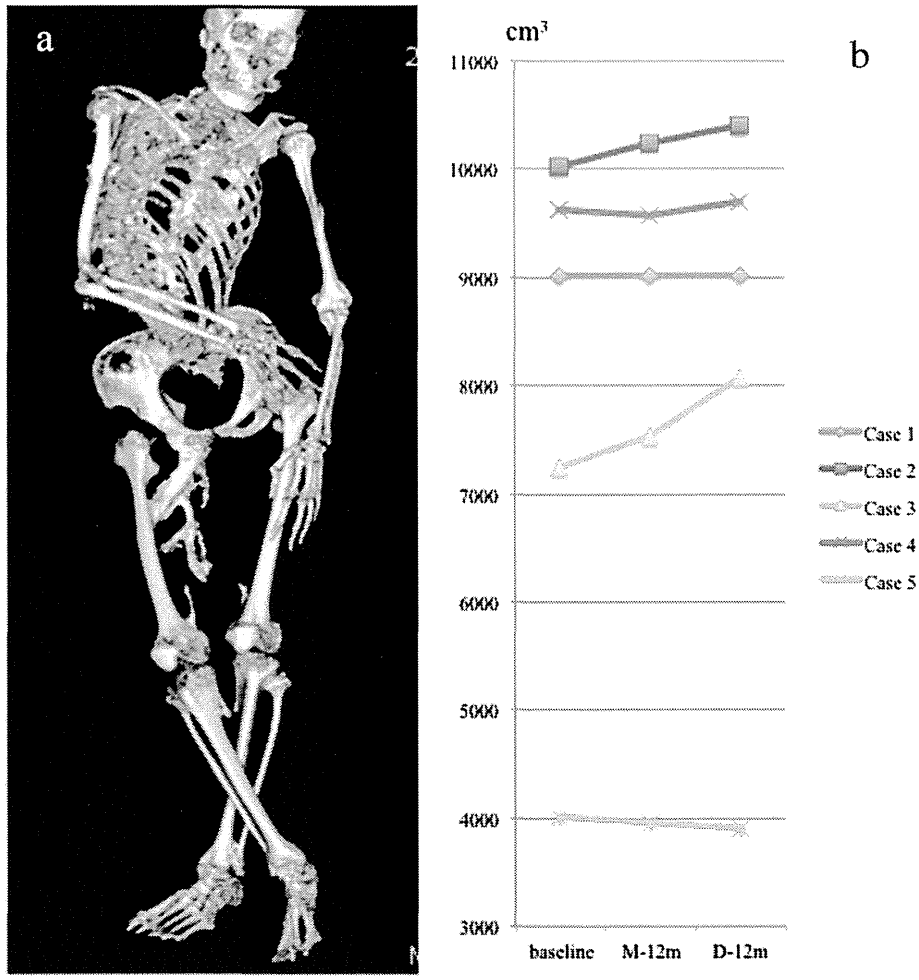

Figure 2 Volumetric computed tomography (CT) examination. Representative reconstructed 3D-CT image obtained by whole body scanning of Case 1 **(a)**, and changes in total bone volume within the region of interests (ROI) in each FOP patient **(b)**. In Case 2, total bone volume has increased 223 cm^3 and 155 cm^3 during the medication and discontinuation phases, respectively. In Case 3, there was an increase of 297 cm^3 and 536 cm^3 in the total bone volume during the medication and discontinuation phases, respectively.

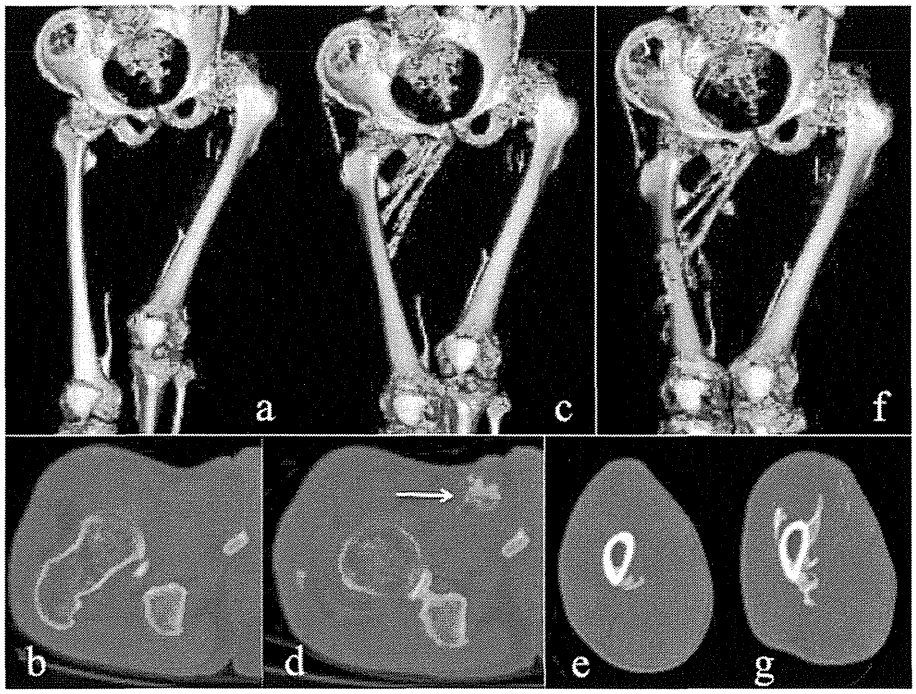

Figure 3 CT images from Case 2. Reconstructed 3D-CT images of the pelvis and bilateral femora at baseline **(a)**, at M-12 m **(c)**, and at D-12 m **(f)**. Axial CT images of the right hip at baseline **(b)**, and at M-12 m **(d)**, and those of the right mid-femur at M-12 m **(e)**, and at D-12 m **(g)**. Heterotopic ossifications in the right adductor muscle (arrow) developed during the medication phase and around mid-femur developed during the discontinuation phase ware clearly demonstrated.

bone volume of 536 cm^3 during the discontinuation phase, which appeared to reflect maturation of the iliopsoas ossification and newly developed bones in the gluteus medius (Figure 4e-g) and around the right jaw joints (Figure 4h,i).

Discussion

To date, there are few clinical trials in the treatment of FOP. Zasloff et al. [14] conducted a prospective study to assess the efficacy of isotretinoin (13-cis-retinoic acid) in the prevention of heterotopic ossification in FOP, and concluded that isotretinoin had no apparent effect in the prevention of new bone formation after surgery or after soft tissue trauma. Brantus and Meunier [15] evaluated the effects of intravenous administration of etidronate and oral corticosteroids for thirty-one FOP attacks in seven patients, and observed 10 new ossifications causing severe deterioration of joint mobility during the mean six years of follow up. These studies indicated that there is no proven efficacy with any therapy in changing the natural history of the disease. Despite the Pex treatment, heterotopic ossification developed rapidly in our two patients suggesting that oral administration of Pex within 0.15-0.60 mg/L seemed to be unsatisfactory in the inhibition of heterotopic ossifications in FOP. Moreover, there is a concerning possibility that Pex administration unexpectedly induced heterotopic ossification in these patients.

Abnormal biochemical measurements of bone mineral metabolism have rarely been reported in FOP [16]. Establishment of useful biomarkers as correlates of disease severity and clinical outcome is desirable to enable early proof-of-concept studies that can help screen potential drug candidates and identify therapeutic targets. Kaplan et al. [17] described that serum ALP activity may increase during disease flare-ups. Our serial clinical and biochemical evaluations demonstrated that elevation of serum ALP and BAP, which synchronized with acute flare-ups, preceded the heterotopic new bone formations. Serum levels of ALP or BAP could be useful biomarkers for monitoring the development of heterotopic ossifications and efficacy of the therapy in FOP.

Multi-detector-row CT has widely been used in clinical environments, and whole body scanning allows 3D structural characterization of entire bone segment at high resolution [18]. Despite the restricted movement and joint immobilization of our patients, standardization of ROI in each individual could allow for accurate volume calculating capabilities. To the best of our

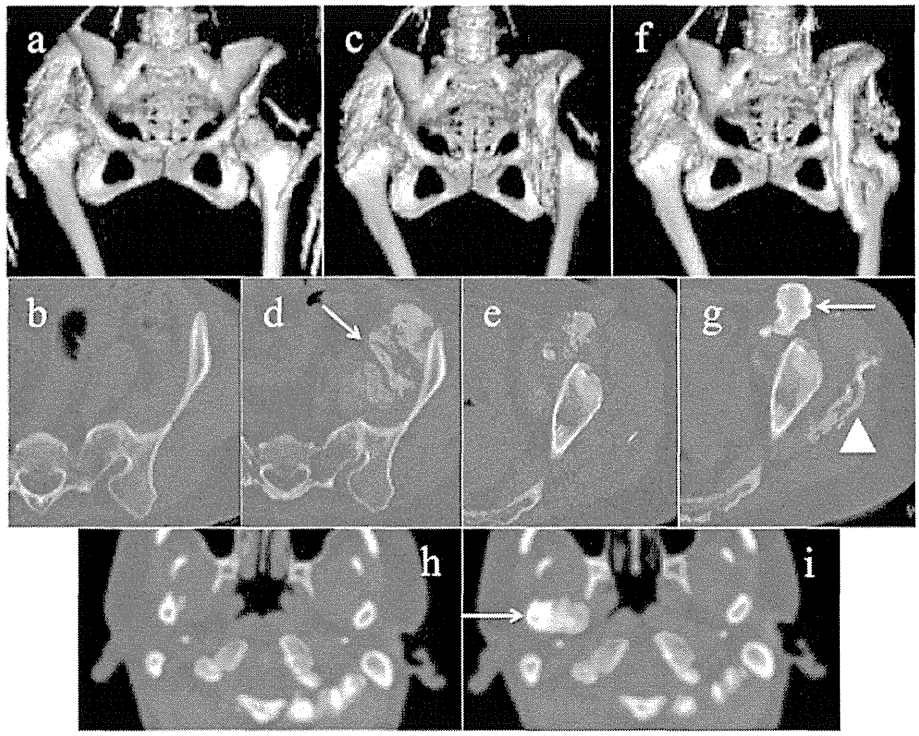

Figure 4 CT images form Case 3. Reconstructed 3D-CT images of the hip joints at baseline **(a)**, at M-12 m **(c)**, and at D-12 m **(f)**. Axial CT images of the left pelvis at baseline **(b)**, at M-12 m **(d, e)**, and at D-12 m **(g)**, and those of the bilateral jaws at M-12 m **(h)**, and at D-12 m **(i)**. Massive new bone formations in the left iliac muscle were developed during the medication phase **(d**, arrow**)**. During the discontinuation phase, the left intra-iliopsoas ossification matured **(g**, arrow**)**, and heterotopic boned in the left gluteus medius **(g**, arrow head**)** and the right jaw joint **(i**, arrow**)** were newly formed.

knowledge, no studies have presented quantitative assessment of ectopic bone formations in FOP. Volumetric 3D-CT analyses demonstrated that change in the total bone volume correlated with the clinical symptoms and laboratory examinations in two patients who showed active flare-ups. Our study highlights greater capabilities of whole body CT scanning as an evaluation tool for disease progression in FOP, especially in assessment of treatment efficacy during forthcoming clinical trials.

There are several major limitations in the present study. First, since there are no better natural history studies for FOP to date, it is difficult to design any clinical trial with meaningful endpoints. Furthermore, we do not know the natural evolution of ectopic bone formations in our patients. Second, the present study could not be designed for pediatric FOP patients because of uncertainty in safety, tolerability, and pharmacokinetics of Pex in the pediatric population. Third, heterotopic ossification in FOP is generally formed via an endochondral ossification process, but we did not confirm heterotopic cartilage formation in our patients. Quantification of total bone volume based on 3D-CT images could be a reliable evaluation tool for assessment of ectopic bone formations, but radiation exposure by CT examination may be a major issue for young patients. Besides, whole body scanning has always been uncomfortable for severely deformed FOP patients, although it takes less than five minutes. Without scanning the whole body, heterotopic ossification following flare-ups (if they occur) could be evaluated by a narrow scan around the flare-ups region. For future clinical trials, standardization of imaging protocol will be expected in evaluating heterotopic bones in FOP.

Conclusions

Although the number of patients is too small to draw reliable conclusions, oral administration of Pex within the safety dose seemed not to be effective in the inhibition of heterotopic ossifications in FOP, despite the absence of significant adverse effects.

Abbreviations

FOP: Fibrodysplasia ossificans progressiva; ACVR1: Activin A receptor type I; ALK2: Activin-like kinase 2; BMP: Bone morphogenetic protein; Pex: Perhexiline maleate; NSAIDs: Nonsteroidal anti-inflammatory drugs; COX-2: Cyclooxygenase-2; CT: Computed tomography; ALP: Alkaline phosphatase; BAP: Bone-specific alkaline phosphatase; OC: Osteocalcin; JSCC: Japan society of clinical chemistry; EIA: Enzyme immunoassay; RIA: Radioimmunoassay;

3D: Three-dimensional; ROI: Regions of interest; IFOPA: International Fibrodysplasia ossificans progressiva association.

Competing interests
The authors declare that they have no competing interests.

Authors' contribution
H Kitoh did most of the patients' follow up, participated in the whole study and drafted the manuscript. MA did the CT interpretations. H Kaneko, MK, MM, IK participated in the clinical trial. JDH and BCS measured plasma concentration of Pex and suggested an optimal dose of Pex administration. KO and NI participated in the design of the study. All authors contributed to elaborating the manuscript. All authors read and approved the final manuscript.

Authors' information
H Kitoh is a member of the Japanese Research Committee on Fibrodysplasia Ossificans Progressiva.

Acknowledgements
This work was supported in partly by Research Committee on Fibrodysplasia Ossificans Progressiva form the Ministry of Health, Labour and Welfare of Japan.

Author details
[1]Department of Orthopaedic Surgery, Nagoya University Graduate School of Medicine, 65 Tsurumai, Showa-ku, Nagoya, Aichi 466-8550, Japan. [2]Department of Radiological Technology, Nagoya University Graduate School of Medicine, 65 Tsurumai, Showa-ku, Nagoya, Aichi 466-8550, Japan. [3]Department of Rehabilitation, Nagoya University Graduate School of Medicine, 65 Tsurumai, Showa-ku, Nagoya, Aichi 466-8550, Japan. [4]Department of Cardiology and Clinical Pharmacology, Queen Elizabeth Hospital, 28 Woodville Road, Woodville, SA 5011, Australia. [5]Division of Neurogenetics, Center for Neurological Diseases and Cancer, Nagoya University Graduate School of Medicine, 65 Tsurumai, Showa-ku, Nagoya, Aichi 466-8550, Japan.

Received: 24 April 2013 Accepted: 13 October 2013
Published: 16 October 2013

References
1. Shore EM, Feldman GJ, Xu M, Kaplan FS: **The genetics of fibrodysplasia ossificans progressiva.** *Clin Rev Bone Miner Metab* 2005, **3**:201–204.
2. Shore EM, Xu M, Feldman GJ, Fenstermacher DA, Cho T-J, Choi IH, Connor JM, Delai P, Glaser DL, Le Merrer M, Morhart R, Rogers JG, Smith R, Triffitt JT, Urtizberea JA, Zasloff M, Brown MA, Kaplan FS: **A recurrent mutation in the BMP type I receptor ACVR1 causes inherited and sporadic fibrodysplasia ossificans progressiva.** *Nat Genet* 2006, **38**:525–527.
3. Kaplan FS, Chakkalakal SA, Shore EM: **Fibrodysplasia ossificans progressiva: mechanisms and models of skeletal metamorphosis.** *Dis Model Mech* 2012, **5**:756–762.
4. Pignolo RJ, Shore EM, Kaplan FS: **Fibrodysplasia ossificans progressiva: Clinical and genetic aspects.** *Orphanet J Rare Dis* 2011, **6**:80.
5. Cohen RB, Hahn GV, Tabas JA, Peeper J, Levitz CL, Sando A, Sando N, Zasloff M, Kaplan FS: **The natural history of heterotopic ossification in patients who have fibrodysplasia ossificans progressiva. A study of forty-four patients.** *J Bone Joint Surg Am* 1993, **75**:215–219.
6. Yu PB, Hong CC, Sachidanandan C, Babitt JL, Deng DY, Hoyng SA, Lin HY, Bloch KD, Peterson RT: **Dorsomorphin inhibits BMP signals required for embryogenesis and iron metabolism.** *Nat Chem Biol* 2008, **4**:33–441.
7. Yu PB, Deng DY, Lai CS, Hong CC, Cuny GD, Bouxsein ML, Hong DW, McManus PM, Katagiri T, Sachidanandan C, *et al*: **BMP type I receptor inhibition reduces heterotopic [corrected] ossification.** *Nat Med* 2008, **14**:1363–1369.
8. Shimono K, Tung WE, Macolino C, Chi AH, Didizian JH, Mundy C, Chandraratna RA, Mishina Y, Enomoto-Iwamoto M, Pacifici M, Iwamoto M: **Potent inhibition of heterotopic ossification by nuclear retinoic acid receptor-gamma agonists.** *Nat Med* 2011, **17**:454–460.
9. Abbott A: **Neurologists strike gold in drug screen effort.** *Nature* 2002, **417**:109.
10. Yamamoto R, Matsushita M, Kitoh H, Masuda A, Ito M, Katagiri T, Kawai T, Ishiguro N, Ohno K: **Clinically applicable antianginal agents suppress osteoblastic transformation of myogenic cells and heterotopic ossifications in mice.** *J Bone Miner Metab* 2013, **31**:26–33.
11. Fukuda T, Kohda M, Kanomata K, Nojima J, Nakamura A, Kamizono J, Noguchi Y, Iwakiri K, Kondo T, Kurose J, Endo K, Awakura T, Fukushi J, Nakashima Y, Chiyonobu T, Kawara A, Nishida Y, Wada I, Akita M, Komori T, Nakayama K, Nanba A, Maruki Y, Yoda T, Tomoda H, Yu PB, Shore EM, Kaplan FS, Miyazomo K, Matsuoka M, *et al*: **Constitutively activated ALK2 and increases SMAD1/5 cooperatively induce bone morphogenetic protein signaling in fibrodysplasia ossificans progressiva.** *J Biol Chem* 2009, **284**:7149–7156.
12. Shah RR, Oates NS, Idle JR, Smith RL, Lockhart JD: **Impaired oxidation of debrisoquine in patients with perhexiline neuropathy.** *Br Med J* 1982, **284**:295–299.
13. *International Fibrodysplasia Ossificans Progressiva Association.* [http://www.ifopa.org/en/living-with-fop-menu/treatment-guidelines.html]
14. Zasloff MA, Roche DM, Crofford LJ, Hahn GV, Kaplan FS: **Treatment of patients who have fibrodysplasia ossificans progressiva with isotretinoin.** *Clin Orthop* 1998, **346**:121–129.
15. Brantus JF, Meunier PJ: **Effects of intravenous etidronate and oral corticosteroids in fibrodysplasia ossificans progressiva.** *Clin Orthop* 1998, **346**:117–120.
16. Blumenkrantz N, Asboe-Hansen G: **Fibrodysplasia ossificans progressiva. Biochemical changes in blood serum, urine, skin, bone, and ectopic ossification.** *Scand J Rheumatol* 1978, **7**:85–89.
17. Kaplan FS, LeMerrer M, Glaser DL, Pignolo RJ, Goldsby RE, Kitterman JA, Groppe J, Shore EM: **Fibrodysplasia ossificans progressiva.** *Best Pract Res Clin Rheumatol* 2008, **22**:191–205.
18. Ptak T, Rhea JT, Novelline RA: **Radiation dose is reduced with a single-pass whole-body multi-detector row CT trauma protocol compared with a conventional segmented method: initial experience.** *Radiology* 2003, **229**:902–905.

doi:10.1186/1750-1172-8-163
Cite this article as: Kitoh *et al.*: Perhexiline maleate in the treatment of fibrodysplasia ossificans progressiva: an open-labeled clinical trial. *Orphanet Journal of Rare Diseases* 2013 **8**:163.

OPEN ACCESS Freely available online

PLOS | ONE

Verapamil Protects against Cartilage Degradation in Osteoarthritis by Inhibiting Wnt/β-Catenin Signaling

Akira Takamatsu[1,2], Bisei Ohkawara[1], Mikako Ito[1], Akio Masuda[1], Tadahiro Sakai[2], Naoki Ishiguro[2], Kinji Ohno[1]*

1 Division of Neurogenetics, Center for Neurological Diseases and Cancer, Nagoya University Graduate School of Medicine, Nagoya, Japan, **2** Department of Orthopaedic Surgery, Nagoya University Graduate School of Medicine, Nagoya, Japan

Abstract

In past years, the canonical Wnt/β-catenin signaling pathway has emerged as a critical regulator of cartilage development and homeostasis. FRZB, a soluble antagonist of Wnt signaling, has been studied in osteoarthritis (OA) animal models and OA patients as a modulator of Wnt signaling. We screened for FDA-approved drugs that induce *FRZB* expression and suppress Wnt/β-catenin signaling. We found that verapamil, a widely prescribed L-type calcium channel blocker, elevated FRZB expression and suppressed Wnt/β-catenin signaling in human OA chondrocytes. Expression and nuclear translocation of β-catenin was attenuated by verapamil in OA chondrocytes. Lack of the verapamil effects in LiCl-treated and FRZB-downregulated OA chondrocytes also suggested that verpamil suppressed Wnt signaling by inducing FRZB. Verapamil enhanced gene expressions of chondrogenic markers of *ACAN* encoding aggrecan, *COL2A1* encoding collagen type II α1, and *SOX9*, and suppressed Wnt-responsive *AXIN2* and *MMP3* in human OA chondrocytes. Verapamil ameliorated Wnt3A-induced proteoglycan loss in chondrogenically differentiated ATDC5 cells. Verapamil inhibited hypertrophic differentiation of chondrocytes in the explant culture of mouse tibiae. Intraarticular injection of verapamil inhibited OA progression as well as nuclear localizations of β-catenin in a rat OA model. We propose that verapamil holds promise as a potent therapeutic agent for OA by upregulating FRZB and subsequently downregulating Wnt/β-catenin signaling.

Citation: Takamatsu A, Ohkawara B, Ito M, Masuda A, Sakai T, et al. (2014) Verapamil Protects against Cartilage Degradation in Osteoarthritis by Inhibiting Wnt/β-Catenin Signaling. PLoS ONE 9(3): e92699. doi:10.1371/journal.pone.0092699

Editor: Chunming Liu, University of Kentucky, United States of America

Received October 2, 2013; **Accepted** February 25, 2014; **Published** March 21, 2014

Funding: This work was supported by Grants-in-Aid from the Ministry of Education, Culture, Sports, Science and Technology (MEXT), the Ministry of Health, Labor and Welfare (MHLW) of Japan, and the Hori Sciences & Arts foundation. The funders had no role in study design, data collection and analysis, decision to publish, or preparation of the manuscript.

Competing Interests: The authors have declared that no competing interests exist.

* E-mail: ohnok@med.nagoya-u.ac.jp

Introduction

Osteoarthritis (OA) is a progressively degenerative joint disorder characterized by degradation of extracellular matrix (ECM) molecules, loss of articular cartilages, and formation of osteophytes. OA causes chronic disability in elderly people and is one of the major health problems worldwide [1]. No rational medical therapy is currently available for OA except for palliative pain control and physiotherapy, before patients require prosthetic joint replacement therapy.

In OA, dysfunction of articular chondrocytes compromises synthesis of ECM and enhances degradation of ECM, which leads to loss of ECM and cartilage degradation. Aggrecan (ACAN) is the most prominent proteoglycan in cartilage, which holds a large amount of water and ions, and confers mechanical elasticity. Collagens, and in particular collagen II, constitute a highly structured fibrillar network that holds spatial arrangement of tissue and provides tensile strength. ECM including ACAN and collagens are degraded by matrix metalloproteinases (MMPs), aggrecanases (ADAMTSs), and other matrix proteases [2,3]. Chondrocytes orchestrate fine-tuned gene expressions of ECM molecules and their catabolic enzymes to achieve tolerance to mechanical stress as well as elasticity of articular cartilages, which is compromised in OA.

Recent studies revealed that bone morphogenetic proteins (BMPs) [4], Indian hedgehog (IHH) [5], the hypoxia-induced signaling [6], and the Wnt/β-catenin signaling [7–9] induce hypertrophic differentiation of chondrocytes and the subsequent aggravation of OA. Indeed, conditional activation of β-catenin in articular chondrocytes in adult mice leads to premature chondrocyte differentiation and development of an OA-like phenotype [10]. In addition, β-catenin stimulates activity of the ECM catabolic enzymes in articular chondrocytes [11]. We thus sought for a modality to suppress Wnt/β-catenin signaling as a potential therapeutic target for OA.

Extracellular antagonists of Wnt, such as the secreted frizzled-related proteins (SFRPs), the dickkopfs (DKKs), and sclerostin (SOST), have been studied in model animals and patients with OA [12–14]. One of the SFRPs, FRZB (also known as SFRP3), is a Wnt antagonist originally identified as a chondrogenic factor in articular cartilage extracts [15]. An amino acid-substituting single nucleotide polymorphism (SNP) in *FRZB* is associated with hip OA [16]. *Frzb*-knockout mice are susceptible to a collagenase-induced OA[12]. FRZB functions as a natural brake on hypertrophic differentiation of articular cartilage [17]. FRZB is thus expected to serve as a potential therapeutic mediator against OA progression.